Surface Science 630 (2014) 254–259

Contents lists available at ScienceDirect

Surface Science

journal homepage: www.elsevier.com/locate/susc

In-situ non-disruptive cleaning of Ge(100) using H_2O_2(g) and atomic hydrogen

Tobin Kaufman-Osborn [a], Kiarash Kiantaj [a], Chorng-Ping Chang [c], Andrew C. Kummel [a,b,*]

[a] Materials Science and Engineering Program, University of California, San Diego, La Jolla, CA 92093, USA
[b] Department of Chemistry and Biochemistry, University of California, San Diego, La Jolla, CA 92093, USA
[c] Applied Materials, Inc., Santa Clara, CA 95054, USA

ARTICLE INFO

Article history:
Received 25 June 2014
Accepted 11 August 2014
Available online 27 August 2014

Keywords:
Germanium
Hydrogen peroxide
Atomic hydrogen
Scanning tunneling microscopy
X-ray photoelectron spectroscopy

ABSTRACT

In-situ gas phase cleaning of the Ge(100) surface was studied at the atomic level using scanning tunneling microscopy (STM) and scanning tunneling spectroscopy (STS) while chemical analysis of the surface was performed using X-ray photoelectron spectroscopy (XPS). High purity H_2O_2(g) dosing removed carbon contamination from an air exposed Ge(100) sample. The oxide formed via H_2O_2(g) dosing was subsequently removed via either atomic hydrogen exposure at 300 °C or 550–700 °C annealing. STM imaging showed an air exposed Ge(100) surface after H_2O_2(g) dosing and 600–700 °C annealing produced a flat and ordered surface while STS verified the density of states (DOS) is equal to that of a Ge(100) surface which has been cleaned via sputter (500 °C) and annealing (700 °C). Combining H_2O_2(g) with atomic hydrogen dosing or annealing removed carbon via oxidation and oxygen via thermal desorption or reduction from an air exposed Ge(100) surface.

1. Introduction

Germanium has drawn significant interest as an alternative material for use in electronic devices as a replacement of conventional silicon based devices due to its high electron and hole mobilities. In order to effectively employ germanium as a replacement for silicon, a non-disruptive cleaning mechanism is needed which leaves the surface atomically flat and defect-free allowing for nucleation in each surface unit cell for gate oxide growth and contact deposition. Many defects that persist on the Ge surface are carbon based. It is well known that carbon contaminants are difficult to remove from a Ge surface and can pin surface steps between terraces on a Ge(100) surface [1,2]. During device fabrication or material deposition, carbon based contaminants can block or act as nucleation sites, change the order of a reaction during growth, or erroneously appear as growth features. For example, any persisting un-reactive defect sites on the Ge surface can increase the required gate oxide thickness needed to maintain low leakage. Therefore, a non-disruptive (i.e. without ion bombardment) method is needed to effectively clean the entire Ge(100) surface.

There are many different methods for preparing a clean and well-ordered Ge(100) surface in ultra-high vacuum (UHV). Most commonly, cyclic sputtering and annealing are used to clean the surface [3–5]. This is usually done with 400–1000 eV Ar + or Ne + at normal to 45° incidence. The final step is high temperature annealing (550–800 °C) in attempt to eliminate damage caused by sputtering. However, either very long duration anneals or very high temperatures are needed to achieve a flat highly ordered surface and to drive any sputter embedded ions out of the surface [6–13].

Alternatively, wet chemical etching followed by formation of a sacrificial oxide passivation layer which desorbs in vacuum at elevated temperatures can be used to form a clean Ge surface. This process results in varying contamination levels and surface roughness depending on the cleaning and passivation methods [1,2,5,14–17]. A Ge buffer layer is sometimes grown after oxide desorption to increase sample cleanliness and order while minimizing roughness [5,17–19].

Purely in-situ chemical cleaning methods followed by high temperature anneals have also been studied to remove carbon contamination from surfaces [20,21]. Both ozone and oxygen plasmas have been shown to successfully reduce carbon contamination; however, even after this treatment, the Ge surface may still have carbon based protrusions [5].

The goal of this study is to develop an understanding of the surface chemistry for a completely in-situ and low temperature non-disruptive method which completely removes all contaminants from an air exposed Ge(100) surface. First, high purity H_2O_2(g) is shown to completely remove carbon contamination from an air exposed Ge surface consistent with formation of volatile carbon oxides and non-volatile germanium oxides. Second, after H_2O_2(g) dosing to remove carbon, atomic hydrogen dosing at 300 °C was shown to remove the germanium oxide formed during H_2O_2(g) cleaning by chemical reduction. Alternatively, H_2O_2(g) treatment followed by a high temperature anneal leaves a flat, ordered, and contaminant-free surface consistent with thermal desorption of germanium oxides. The cleanliness and

---

* Corresponding author.
E-mail address: akummel@ucsd.edu (A.C. Kummel).

http://dx.doi.org/10.1016/j.susc.2014.08.015
0039-6028/© 2014 Elsevier B.V. All rights reserved.

ordering of the surface were verified using in-situ X-ray photoelectron spectroscopy (XPS), scanning tunneling microscopy (STM), and scanning tunneling spectroscopy (STS).

2. Experimental details

Sb-doped n-type Ge(100) wafers (0.005–0.020 Ωcm, Wafer World Inc.) were diced into 12 mm × 4.5 mm pieces and degreased via ultrasonication with acetone, methanol, and deionized water then dried with N_2 gas. The Ge samples were quickly (<10 min) introduced into the UHV chamber with a base pressure of 2×10^{-10} Torr and degassed via a pyrolytic boron nitride (PBN) heater at 400 °C. After sample loading into the UHV chamber, all sample dosing, processing, and analyzing were carried out in-situ without breaking vacuum. The samples were subsequently transferred into a separate "dosing" chamber with a base pressure of 2×10^{-8} Torr in order to clean the Ge surfaces. The reaction pressures were measured using a convectron gauge, and the exposure was estimated in Langmuirs (1 Langmuir (L) $= 1 \times 10^{-6}$ Torr · 1 s).

After loading the Ge(100) samples into the "dosing" chamber, the samples were exposed to high purity $H_2O_2(g)$ while the sample temperature was maintained at 300 °C via resistive heating with a PBN heater. The high purity $H_2O_2(g)$ source is built by RASIRC® and is maintained at 40 °C. The $H_2O_2(g)$ source uses 30% $H_2O_2(aq)$ solution and greatly reduces any contamination in the $H_2O_2(g)$ delivery (i.e. contamination from adsorbed gases in the liquid). Glass and Teflon tubing were employed in order to minimize $H_2O_2(g)$ decomposition on the tubing or stainless steel dosing chamber. The reported doses of $H_2O_2(g)$ in Langmuir are presented assuming a 0% dissociation rate of $H_2O_2(g)$.

After high purity $H_2O_2(g)$ dosing, the samples were given one of two treatments to remove the oxide formed during $H_2O_2(g)$ dosing. The samples were either dosed with atomic hydrogen at modest temperatures, 300 °C, to chemically reduce the oxide, or annealed at high temperature, up to 700 °C, to desorb the oxide. For oxide removal via atomic hydrogen plasma, the samples were transferred into the "dosing" chamber and exposed to an atomic hydrogen plasma while the sample temperature was maintained at 300 °C. The atomic hydrogen plasma was generated in an Opthos McCarroll cavity using a microwave generator (Sairem Model GMP 03 K/SM). Inside of the McCarroll cavity, the plasma was generated in either a quartz (see supplemental materials) or sapphire discharge tube with a power of 30 W. The pressure during dosing of atomic hydrogen was ~300 mTorr and the dosing gas was composed of 5% $H_2(g)$ and 95% Ar(g). The atomic H doses reported assume 100% dissociation and, therefore, only represent an upper limit. For oxide desorption via heating, samples were heated via direct heating in the UHV chamber using a controlled heating ramp rate of 1 °C/s while the sample temperature was monitored by a pyrometer. GeO is known to desorb from the Ge(100) surface starting around 400 °C for submonolayer coverage while GeO_2 will decompose into GeO and desorb between 550 and 600 °C [22–24].

In-situ analysis of the sample surface was conducted after each surface treatment. A monochromatic XPS (XM 1000 MkII/SPHERA, Omicron Nanotechnology) was employed to examine the surface elements and their relative intensities. The XPS data was acquired in constant analyzer energy mode with a pass energy of 50 eV and a step size of 0.1 eV using an Al Kα source (1486.7 eV). XPS spectra were collected with a takeoff angle of 30° from the sample surface (i.e. close to the surface parallel) with an acceptance angle of $\pm 7°$. Analysis of the spectra was performed using CASA XPS v.2.3 using a Shirley background subtraction method. The relative XPS elemental intensities were quantified by calculating the peak area divided by the XPS relative sensitivity factor. The elemental ratios reported display the best fit of the data while the reported errors bars represent the largest deviations of potential fits of the spectra. The topographical analysis of the sample surfaces was performed using a STM (LT-STM, Omicron Nanotechnology). All STM and STS data were obtained at room temperature (RT) in a UHV chamber with a base pressure of 1×10^{-11} Torr. The STM was operated in constant-current mode ($I_{sp} = 0.2$ nA) with an applied sample bias of -1.8 V. The electronic structure of the surfaces of the samples was measured using STS operating in variable-z mode using a modulation signal (0.1 V, 650 Hz) supplied by an external lock-in amplifier while sweeping the sample bias from -1 to $+1$ V.

3. Results and discussion

3.1. Chemical analysis: XPS results

Fig. 1 shows the relative elemental ratios acquired via XPS of carbon (black) and oxygen (red) contaminants normalized to the Ge signal on a Ge(100) sample after several surface treatments. Column A shows the ratios of contaminants to germanium of a Ge(100) sample after ex-situ degreasing and subsequent air exposure during sample transfer and loading into the chamber. The degreased Ge(100) sample (Fig. 1, Column A) has a multilayer coverage of carbon and oxygen contaminant on the surface due to hydrocarbon and water adsorption during air exposure. After degassing the sample at 400 °C (Column B), all of the oxygen and native oxide desorbed from the sample consistent with the dominant ambient Ge oxide, formed during short air exposure (<10 min), being a suboxide (see XPS chemical shift data below); however, some remaining carbon contamination persists on the surface. Column C shows the carbon and oxygen on the sample after a subsequent 20 second exposure of high purity $H_2O_2(g)$ at 300 mTorr (6×10^6 L) while the sample temperature was maintained at 300 °C. $H_2O_2(g)$ reacts with carbon on the surface forming volatile carbon and reaction by-products which readily desorbed at 300 °C reducing the carbon signal in XPS while also forming a germanium oxide (Column C) (see XPS chemical shift data below). Subsequently, heating the sample to 700 °C desorbed the oxide formed during $H_2O_2(g)$ dosing eliminating oxygen contamination on the surface while the carbon signal does not change (Column D). The 20 second high purity $H_2O_2(g)$ dose at 300 mTorr (6×10^6 L) + 700 °C anneal was repeated (Column E) and showed a decrease of carbon. To accelerate the carbon removal, the $H_2O_2(g)$ dose was increased. Column F shows a contaminant free surface after an additional 80 second (2 min total or 3.6×10^7 L) of

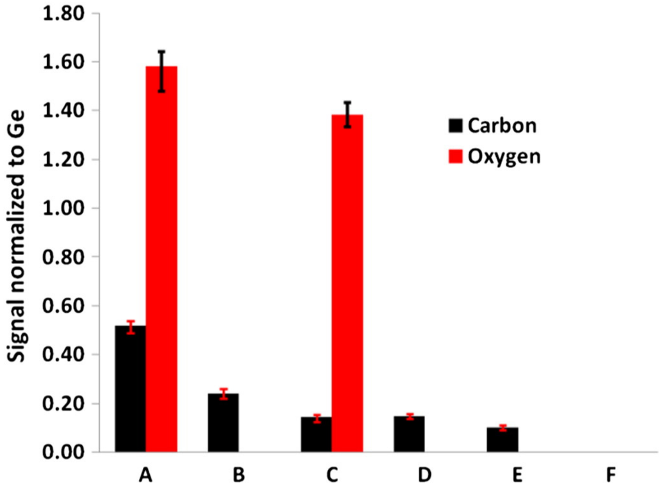

Fig. 1. XPS elemental ratios of carbon and oxygen on a Ge(100) surface during cleaning. XPS showing carbon and oxygen reduction following dosing of high purity $H_2O_2(g)$ and 700 °C annealing. Column A shows ratios on an as-loaded Ge(100) sample. Column B shows ratios after 400 °C degassing. Column C shows ratios after a subsequent 20 s dose of $H_2O_2(g)$. Column D shows ratios after a subsequent 700 °C anneal. Column E shows ratios after an additional 20 s dose of $H_2O_2(g)$ and subsequent 700 °C anneal. Column F shows a contaminant free surface after additional 80 s (2 min total) $H_2O_2(g)$ dose and subsequent 700 °C anneal. (For interpretation of the references to color in this figure legend, the reader is referred to the web version of this article.)

high purity $H_2O_2(g)$ dosing (300 mTorr) at 300 °C followed by a 700 °C anneal.

Fig. 2 shows the progression of the carbon signal in XPS after the $H_2O_2(g) + 700$ °C anneal cleaning procedure. The air exposed sample shows a carbon peak with a large feature with binding energy near 284.5 eV consistent with hydrocarbons or Ge–C (orange peak) and also a broad higher binding energy peak (blue) near 286.5 eV consistent with C–O bonding[25–27]. When the sample is degassed at 400 °C, the carbon signal decreased consistent with C–O desorption (reduction in higher binding energy blue peak) while the hydrocarbon/Ge–C feature persists. After a 20 second dose of $H_2O_2(g)$, the higher binding energy feature (C–O bonding) is completely eliminated while the hydrocarbon/Ge–C feature (284.5 eV) is reduced. The subsequent 700 °C anneal has no impact on the carbon signal. After a subsequent 20 second $H_2O_2(g)$ dose + 700 °C anneal, the carbon peak is further decreased. A additional 80 s $H_2O_2(g)$ dose (2 min total or 3.6×10^7 L) followed by a 700 °C anneal shows a completely carbon free surface consistent with removal of both hydrocarbons/Ge–C and C–O.

Fig. 3 shows the progression of the Ge 3d peak during the cleaning process. The degreasing step ending with a water rinse completely dissolved the GeO_2 native oxide that formed during extended air exposure [1]. The air exposed (<10 min air exposure) sample shows a Ge bulk peak (green curve) near 29.5 eV and also a higher binding energy peak near 31.7 eV consistent with a native oxide formed during short air exposure being GeO_x ($x < 2$) (red curve). It is known that GeO_2 will slowly form on the clean Ge surface after long exposure times (on the order of hours to days) [28,29]. In addition, the binding energy of GeO_2 is at 32.8–33.2 eV verifying that the majority of the native oxide formed during air exposure during transfer from degreasing to UHV chamber is suboxide [28,30,31]. After degassing the sample at 400 °C, the GeO_x ($x < 2$) feature is completely eliminated and the XPS spectrum shows only a Ge bulk feature. Note that this bulk-like peak does not show the Ge–C feature because the carbon contamination level is below the signal to noise ratio of this spectrum. After 20 s of $H_2O_2(g)$ dosing to remove carbon from the surface, the high binding energy feature (ranging from 30.6 to 33.2 eV) returns. This higher binding energy feature is fit with one broad peak which encapsulates the variety of different binding energies (germanium oxidation states) due to many potential bonding configurations after $H_2O_2(g)$ dosing (Ge–OH, GeO, Ge_2O_3, GeO_2); therefore, it is referred to as GeO_xH_y ($x \leq 2, 0 \leq y \leq 1$) (red curve) [32]. A 700 °C anneal completely desorbs the GeO_xH_y feature leaving only a bulk Ge feature. Subsequent $H_2O_2(g)$ dosing and annealing further decrease the carbon contamination on the surface as seen in Figs. 1 & 2 while the Ge 3d spectra only show a bulk Ge feature after each 700 °C anneal.

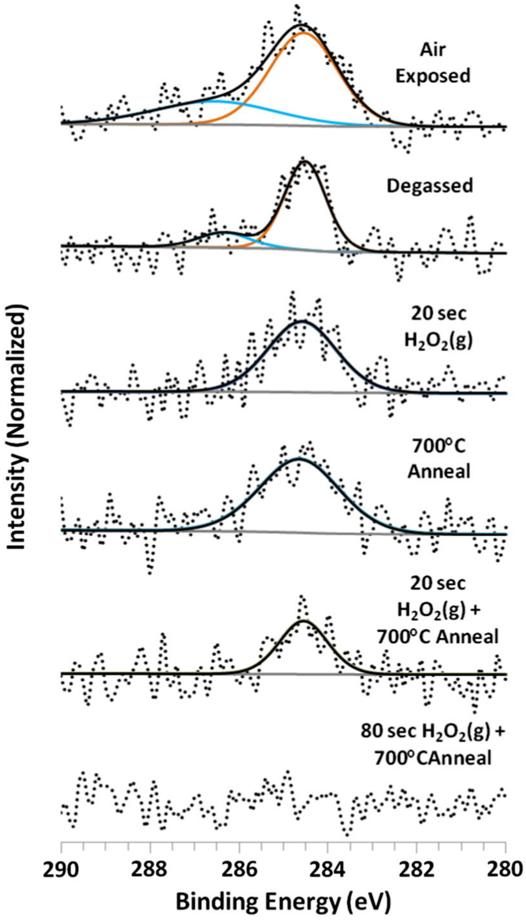

Fig. 2. XPS carbon 1s spectra during $H_2O_2(g)$ dosing and annealing. Carbon 1s spectra during cleaning procedure involving $H_2O_2(g)$ dosing and 700 °C annealing corresponding with procedure outlined in Fig. 1. (For interpretation of the references to color in this figure legend, the reader is referred to the web version of this article.)

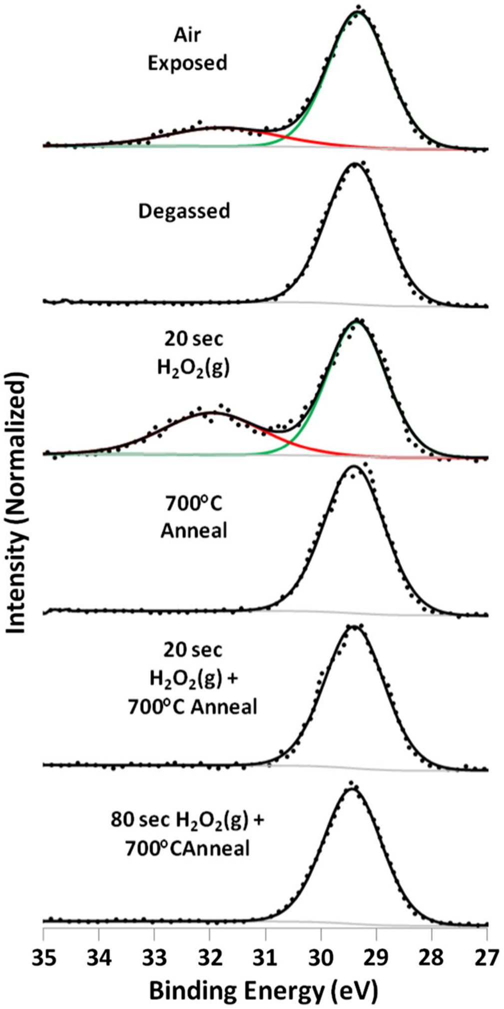

Fig. 3. XPS Ge 3d spectra during $H_2O_2(g)$ dosing and annealing. Ge 3d spectra during the cleaning procedure involving $H_2O_2(g)$ dosing and 700 °C annealing corresponding with procedure outlined in Figs. 1 & 2. (For interpretation of the references to color in this figure legend, the reader is referred to the web version of this article.)

In order to reduce the thermal budget required for obtaining a contaminant free Ge(100) surface, a chemical reduction was investigated which removes oxygen from the surface at a lower temperature. Fig. 4 shows the XPS contaminant:Ge ratios of the $H_2O_2(g)$ dosed Ge(100) surface followed by atomic H dosing. As noted in the supplemental

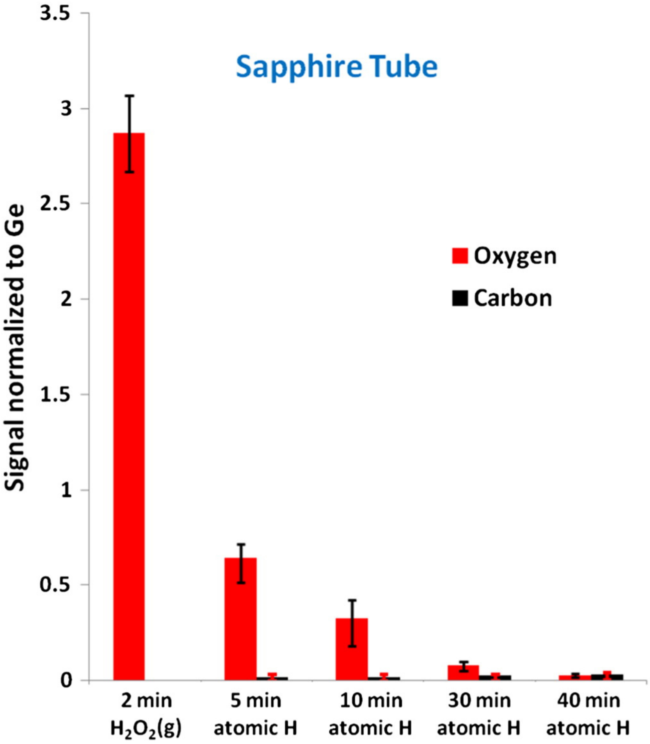

Fig. 4. XPS elemental ratio of oxygen and carbon during H_2O_2(g) and subsequent atomic hydrogen dosing (sapphire discharge tube). XPS showing oxygen on the Ge(100) surface after 2 min of H_2O_2(g) cleaning followed by increasing exposure to atomic hydrogen generated in a sapphire discharge tube. Atomic hydrogen reduces oxygen contamination down to <2% on the Ge(100) surface.

materials, a sapphire tube rather than a quartz tube is required for low oxygen contamination because atomic hydrogen generation inside a quartz tube results in etching of the quartz and oxygen deposition onto the sample. Fig. 4 shows the amount of oxygen and carbon on the Ge(100) surface after a 2 min exposure to high purity H_2O_2(g) (300 mTorr, 300 °C, 3.6 × 10^7 L). As previously shown, a 2 min H_2O_2(g) dose was able to completely strip all carbon contaminants from an air exposed Ge(100) surface (Fig. 1 Column F) and the carbon contamination level during the entire atomic H dosing procedure remained consistently below 3%. This carbon contamination is attributed to background oil vapor from a mechanical pump. The Ge(100) sample was subsequently dosed with atomic H for increasing exposure times while the sample temperature was maintained at 300 °C. Fig. 4 shows a ~2.8:1 O:Ge ratio after a 2 min high purity H_2O_2(g) dose. Exposure estimates for atomic hydrogen dosing are presented assuming a 100% dissociation of the 5% H_2(g) in the gas mixture. After a 5 minute exposure to 300 mTorr of the gas mixture (9 × 10^6 L of atomic hydrogen), the O:Ge ratio was decreased by a factor of 4. Increasing the exposure time of atomic hydrogen to 10 min (1.8 × 10^7 L), 30 min (5.4 × 10^7 L), or 40 min (7.2 × 10^7 L) demonstrates the ability to remove oxygen contaminants down to <2% compared to the Ge signal. In contrast to the plasma generated in the quartz discharge tube (see supplemental material), the plasma from the sapphire discharge tube minimizes the oxygen contamination on the Ge(100) surface.

Fig. 5 shows the progression of the Ge 2p peak after the 2 min H_2O_2(g) dose and subsequent atomic hydrogen dosing. The Ge 2p peak after a 2 min H_2O_2(g) dose (300 mTorr, 300 °C, 3.6 × 10^7 L) has a dominant oxide feature (red curve) between 1219 and 1222 eV consistent with a variety of potential bonding configurations including Ge – OH, GeO, Ge_2O_3, and GeO_2. After 5 min of atomic H dosing (9 × 10^6 L, 300 °C, 300 mTorr), the oxide peak is reduced while the germanium bulk signal (green curve) increases. After 10 min of atomic H dosing (1.8 × 10^7 L, 300 °C, 300 mTorr), the oxide feature decreases while the bulk feature continues to increase. Also, the oxide feature shifts to a slightly lower binding energy indicating a preferential reduction of the GeO_2 oxide. 30 min of atomic H dosing (5.4 × 10^7 L, 300 °C, 300 mTorr) further decreases the oxide feature as it shifts to a lower binding energy demonstrating significant reduction of oxygen off the surface. After a total of 40 min of atomic H dosing (7.2 × 10^7 L, 300 °C, 300 mTorr) the higher binding energy feature (red curve) is almost completely eliminated indicating successful removal of contaminants off the Ge(100) surface.

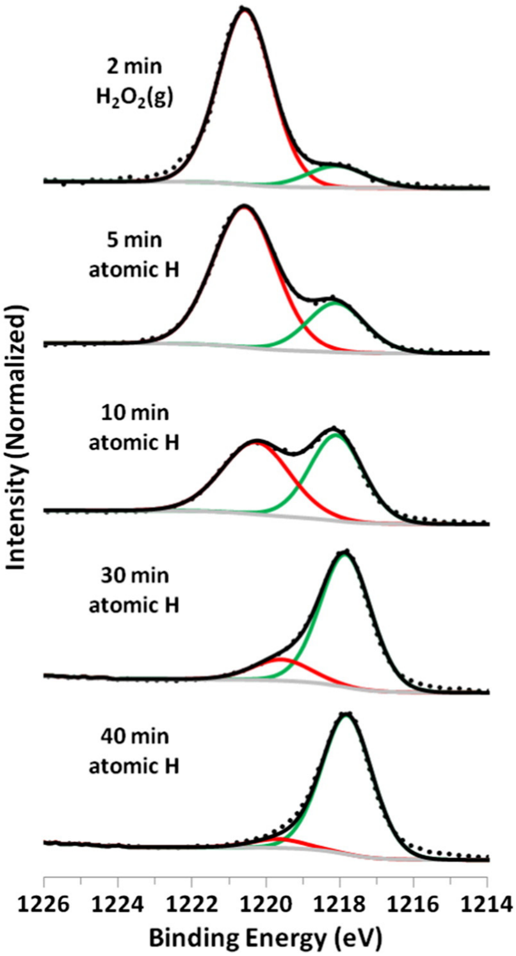

Fig. 5. XPS Ge 2p spectra during H_2O_2(g) dosing followed by atomic hydrogen dosing. Ge 2p spectra during the cleaning procedure involving H_2O_2(g) dosing and subsequent atomic hydrogen dosing corresponding with the procedure outlined in Fig. 4. (For interpretation of the references to color in this figure legend, the reader is referred to the web version of this article.)

3.2. Topographical and electronic analysis: STM & STS results

While H_2O_2(g) + atomic hydrogen dosing forms a contaminant free surface, in order to form a well-ordered surface with low roughness, higher annealing temperatures are required. In order to better analyze the quality of the Ge(100) surface after contaminant removal, STM and STS were implemented. STM requires long range order and long range surface flatness to obtain atomically resolved images over large regions due to the relative bluntness of the tip. Multiple STM studies were performed with lower temperature anneals and atomic order could only be observed in small regions; long range order required a >600 °C anneal.

Fig. 6 shows an STM image of a Ge(100) sample cleaned via H_2O_2(g) and subsequently annealed at 700 °C for 5 min (Fig. 6A) or 600 °C for 1 h (Fig. 6C). The topography is compared to a sputter and

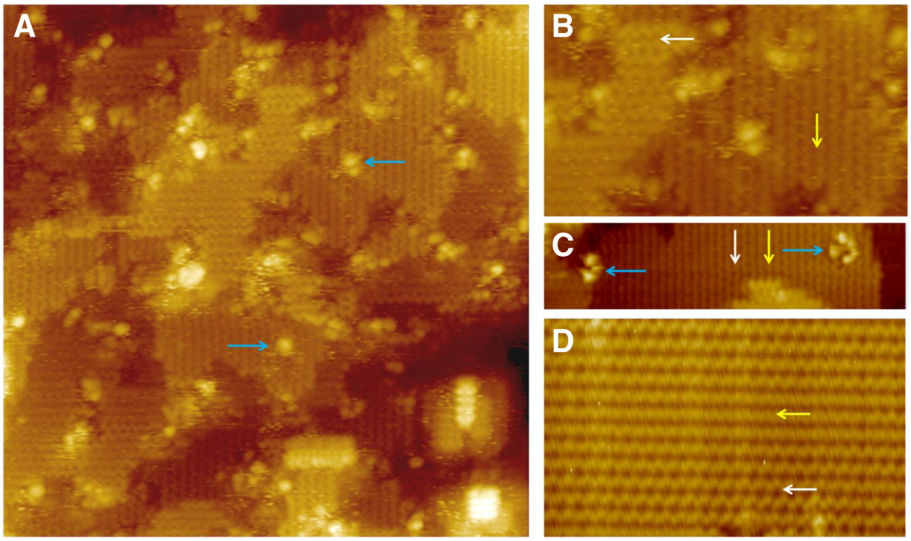

Fig. 6. STM of a Ge(100) surface cleaned via H_2O_2(g) dosing + annealing or sputtering and annealing (A) 40 × 40 nm^2 STM image of the Ge(100) surface after H_2O_2(g) dosing and 700 °C annealing (5 min). A large amount of ordering is observed while a few Ge adatoms (blue arrows) sit atop some terraces. (B) 20 × 10 nm^2 inset of Ge(100) surface shown in (A) highlighting ordering and (2 × 1) (yellow arrow) and c(4 × 2) (white arrow) reconstructions. (C) 20 × 10 nm^2 STM image of the Ge(100) surface after H_2O_2(g) dosing and 600 °C annealing (60 min). (D) 20 × 10 nm^2 STM image of a Ge(100) cleaned via sputter and 700 °C annealing showing (2 × 1) (yellow arrow) and c(4 × 2). (For interpretation of the references to color in this figure legend, the reader is referred to the web version of this article.)

annealed Ge(100) surface (Fig. 6D). Longer duration anneals are required to achieve increased surface ordering needed for STM and STS, especially at lower temperatures. H_2O_2(g) dosing followed by 700 °C annealing produced a flat surface with a 0.17 nm RMS (root mean squared) roughness over 100 × 100 nm. A typical Ge(100) sample that was thoroughly sputtered and annealed has an average 0.13 nm RMS roughness over 100 × 100 nm. However, the sputter and annealing treatment requires repeated long duration (30 min) 700 °C anneals to eliminate damage caused via ion bombardment. Long duration high temperature anneals are not compatible with device fabrication and insufficient annealing would result in high surface roughness which would lower electron and hole mobilities. The H_2O_2(g) + <600 °C anneal cleaned surface shows large amounts of atomic order with no large etch pits and a small percentage of Ge adatoms (<5% of the surface) sit on top of terraces (highlighted by blue arrows). The carbon signal on these surfaces are below the detection level of XPS and the characteristic (2 × 1) (yellow arrow) and c(4 × 2) (white arrow) reconstructions seen on the sputtered/annealed Ge(100) surface are also seen in the H_2O_2(g) dosed + >600 °C anneal cleaned surfaces (in Fig. 4b & c). The adatoms on the 700 °C annealed surface and larger RMS roughness compared to a sputtered/annealed sample are most likely caused by insufficient annealing.

Line trace analysis (Fig. 7A) taken at 5 different locations (each line trace offset by 100 nm) on the chemically cleaned surface (Fig. 6A) shows periodic row spacing of 7.9 Å with a standard error of .1 Å which is nearly identical to the row spacing on the ideal clean Ge(100) surface (8 Å) [33]. STS verifies that the electronic structure (density of states) of the surface after this cleaning procedure is equivalent to that produced using sputter and annealing as seen by the strong agreement of the bandgaps of the orange and blue STS curves in Fig. 7B. The difference in signal strength in the negative sample bias is only an artifact of normalization. The alignment of the band gap and Fermi level position agreement is more indicative of agreement in the surface density of states. The data is consistent with the 600–700 °C anneal being required to restore surface order since the GeO_x desorbs at >400 °C leaving a slightly rougher surface.

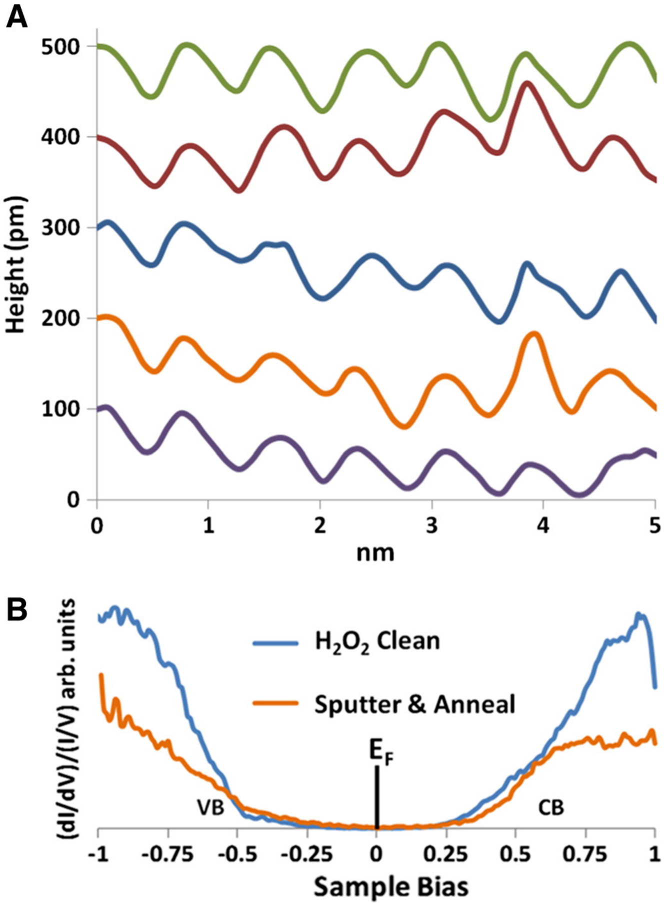

Fig. 7. Line trace analysis and STS of the chemically cleaned Ge(100) surface. (A) Line trace analysis acquired at five different locations on the chemically cleaned Ge(100) surface (Fig. 6A) showing periodic row spacing of 7.9 Å with a standard error of .1 Å. (B) STS acquired on the chemically cleaned Ge(100) surface compared to a sputter/anneal cleaned Ge(100) surface showing identical DOS.

4. Conclusion

Air exposed Ge(100) samples were cleaned of surface contaminants using high purity H_2O_2(g) followed by either atomic hydrogen dosing at 300 °C or a high temperature anneal (550 °C–700 °C). High purity

H_2O_2(g) dosed on an air exposed surface at 300 °C reacted with carbonaceous species on the surface forming volatile compounds. The H_2O_2(g) dosing removed all the carbon contamination on the Ge(100) surface while also forming a GeO_xH_y layer. The oxide formed during H_2O_2(g) dosing can be removed via reduction by one of two methods: annealing or atomic H dosing. Atomic hydrogen dosing reduced the germanium oxide layer forming volatile by-products at 300 °C thereby removing oxygen from the surface. While H_2O_2(g) + atomic H dosing is successful at removing all contaminants from the Ge(100) surface, STM verifies that a 600–700 °C anneal leaves a flat and ordered Ge(100) surface. STS verified that the high temperature annealed surface has a density of states on the surface equivalent to that of a sample cleaned via sputter and annealing.

Acknowledgements

This work was supported by the Semiconductor Research Corporation (Task 2051.001) in coordination with Applied Materials (Task 2181.001) and Global Foundries (2451.001). The authors would like to acknowledge RASRIC® for providing the high purity H_2O_2(g) source.

Appendix A. Supplementary data

Supplementary data to this article can be found online at http://dx.doi.org/10.1016/j.susc.2014.08.015.

References

[1] J.S. Hovis, R.J. Hamers, C.M. Greenlief, Surf. Sci. 440 (1999) L815.
[2] S. Gan, L. Li, T. Nguyen, H. Qi, R. Hicks, M. Yang, Surf. Sci. 395 (1998) 69.
[3] A. Wachs, T. Miller, T. Hsieh, A. Shapiro, T.-C. Chiang, Phys. Rev. B 32 (1985) 2326.
[4] H. Zandvliet, A. Van Silfhout, Surf. Sci. 195 (1988) 138.
[5] L. Chan, E. Altman, Y. Liang, J. Vac. Sci. Technol. A 19 (2001) 976.
[6] R. Bringans, H. Höchst, Phys. Rev. B 25 (1982) 1081.
[7] L. Surnev, Surf. Sci. 110 (1981) 439.
[8] J. Aarts, A. Hoeven, P. Larsen, Phys. Rev. B 37 (1988) 8190.
[9] G. Schulze, M. Henzler, Surf. Sci. 73 (1978) 553.
[10] J. Lander, J. Morrison, J. Appl. Phys. 34 (2004) 1403.
[11] R. MacDonald, D. Haneman, J. Appl. Phys. 37 (2004) 1609.
[12] W. Yang, X. Wang, K. Cho, J. Kishimoto, S. Fukatsu, T. Hashizume, T. Sakurai, Phys. Rev. B 50 (1994) 2406.
[13] S. Kevan, Phys. Rev. B 32 (1985) 2344.
[14] K. Prabhakarana, T. Ogino, R. Hull, J. Bean, L. Peticolas, Surf. Sci. 316 (1994) L1031.
[15] T. Akane, J. Tanaka, H. Okumura, S. Matsumoto, Appl. Surf. Sci. 108 (1997) 303.
[16] H. Okumura, T. Akane, S. Matsumoto, Appl. Surf. Sci. 125 (1998) 125.
[17] W. Klesse, G. Scappucci, G. Capellini, M. Simmons, Nanotechnology 22 (2011) 145604.
[18] K. Horn, J. Tsao, E. Chason, D. Brice, S. Picraux, J. Appl. Phys. 69 (1991) 243.
[19] J.E. Van Nostrand, S.J. Chey, M.-A. Hasan, D.G. Cahill, J. Greene, Phys. Rev. Lett. 74 (1995) 1127.
[20] X.J. Zhang, G. Xue, A. Agarwal, R. Tsu, M.A. Hasan, J. Greene, A. Rockett, J. Vac. Sci. Technol. A 11 (1993) 2553.
[21] S. Gan, Y. Liang, D.R. Baer, Surf. Sci. 459 (2000) L498.
[22] S.K. Wang, K. Kita, C.H. Lee, T. Tabata, T. Nishimura, K. Nagashio, A. Toriumi, J. Appl. Phys. 108 (2010) 054104.
[23] D.A. Hansen, J.B. Hudson, Surf. Sci. 292 (1993) 17.
[24] K. Kita, S. Wang, M. Yoshida, C. Lee, K. Nagashio, T. Nishimura, A. Toriumi, Comprehensive study of GeO 2 oxidation, GeO desorption and GeO 2-metal interaction-understanding of Ge processing kinetics for perfect interface control, IEEE, 2009. 1.
[25] P. Merel, M. Tabbal, M. Chaker, S. Moisa, J. Margot, Appl. Surf. Sci. 136 (1998) 105.
[26] C. Wagner, W. Riggs, L. Davis, J. Moulder, G. Muilenberg, Eden Prairie, MN, 1979. 152.
[27] N. Tabet, M. Faiz, N. Hamdan, Z. Hussain, Surf. Sci. 523 (2003) 68.
[28] K. Prabhakaran, T. Ogino, Surf. Sci. 325 (1995) 263.
[29] T. Deegan, G. Hughes, Appl. Surf. Sci. 123 (1998) 66.
[30] D. Schmeisser, R. Schnell, A. Bogen, F. Himpsel, D. Rieger, G. Landgren, J. Morar, Surf. Sci. 172 (1986) 455.
[31] K.-i. Seo, P.C. McIntyre, S. Sun, D.-I. Lee, P. Pianetta, K.C. Saraswat, Appl. Phys. Lett. 87 (2005) (042902-042902-3).
[32] S. Swaminathan, Y. Oshima, M.A. Kelly, P.C. McIntyre, Appl. Phys. Lett. 95 (2009) (032907-032907-3).
[33] H.J. Zandvliet, Phys. Rep. 388 (2003) 1.